# Density-functional calculation of the parameters in the Anderson model: Application to Mn in CdTe

O. Gunnarsson, O. K. Andersen, O. Jepsen, and J. Zaanen

*Max-Planck-Institut für Festkörperforschung, Postfach 800 665, D-7000 Stuttgart 80, West Germany*

(Received 26 April 1988)

We discuss methods for *ab initio* calculations of the parameters in the Anderson model. First, we present a very simple method for calculating the appropriate combination of hopping matrix elements needed in the impurity Anderson model. For a substitutional impurity, we show that to a good approximation it is sufficient to know the potential of the impurity atom and the local density of states of the unperturbed host. Calculations are performed for Mn substituting Cd in CdTe. As expected, the Mn $3d$ orbitals have a strong coupling to the Te $5p$–derived valence band, but there is also a strong coupling to the conduction band. The dependence of the hopping matrix elements on the Mn configuration is studied. While there is a strong dependence on the Mn net charge, we find that the creation of, e.g., a core hole has a fairly small effect on the matrix elements, provided that the $3d$ occupancy is allowed to relax. Second, the Coulomb integrals between two Mn $3d$ orbitals and between a $3d$ orbital and a core orbital are calculated. The renormalization of these quantities due to the radial relaxation of the Mn $3d$, $4s$, and $4p$ orbitals, and due to charge-transfer effects, are analyzed in detail. Because of the nonmetallic character of CdTe, a change in the number of Mn $3d$ electrons is only partly screened by a charge transfer to the Mn $4s$ and $4p$ orbitals. Because of the moderate size of the band gap, this screening is, nevertheless, important. The radial relaxation of the Mn $3d$, $4s$, and $4p$ wave functions is also important. The relaxation of the neighboring atoms plays a rather small role. Results for the photoemission spectra are calculated including multiplet effects. The results are found to be in rather good agreement with experiment.

## I. INTRODUCTION

The Anderson impurity model[1] has been found to provide a satisfactory description of different properties of many systems, which have a localized state interacting with a continuum of extended states. Examples of such systems are rare-earth compounds [e.g., Ce (Refs. 2–4) and Yb (Ref. 5) compounds], actinide compounds (e.g., some light oxides[6]), $3d$ compounds,[7–9] and chemisorption systems.[10] The Anderson model is defined by the Hamiltonian

$$H = \sum_{k,\sigma} \varepsilon_k n_{k\sigma} + \sum_{m,\sigma} \varepsilon_m n_{m\sigma} + \sum_{k,m,\sigma} (V_{km} \psi_{m\sigma}^{\dagger} \psi_{k\sigma} + \text{H.c.})$$
$$+ \tfrac{1}{2} U \sum_{m,m,'\sigma,\sigma'}{}' n_{m\sigma} n_{m'\sigma'} . \tag{1}$$

In this model we have divided the complete orthonormal set of one-electron functions into two subsets. One set is given by the localized orbitals, labeled by the azimuthal quantum number $m$ and spin index $\sigma$, and with the energies $\varepsilon_m$. The other set consists of states with energies $\varepsilon_k$ and labeled by some quantum number $k$ and spin $\sigma$. The localized states have a strong Coulomb interaction $U$, which must be taken into account explicitly using some many-body technique to solve model (1). The set of states $|k\sigma\rangle$, on the other hand, is assumed to be extended and the Coulomb interaction between these states is not included explicitly. The one-particle part of the Hamiltonian is assumed to have been diagonalized in the space of states $|k\sigma\rangle$, and we are only left with the hopping matrix

elements $V_{km}$ between the two sets of states. To obtain the proper multiplet structure, we, in addition, have to add $m$-dependent Coulomb integrals, which will, however, not be discussed further here. For the description of core spectroscopies, a further term is added to the Hamiltonian in (1) to describe the Coulomb interaction $U_c$ between the core and the localized states.[7]

All other interactions are usually neglected in the Anderson model, although they are in general not small. Basic assumptions in the model are that such interactions can, nevertheless, be included implicitly as a renormalization of the parameters, and that this renormalization is the same for different experiments. The normal approach has been to determine the parameters of the model empirically, requiring that the parameters are chosen so that some experiment, for instance, core-level x-ray photoemission spectroscopy (XPS) is well described. These parameters are then used to describe other properties. In particular for Ce compounds there have been extensive tests, showing that this approach can be quite successful.[2–4] While such an empirical approach includes renormalization effects, it gives little information about the origin or size of the renormalization.

It would be desirable to be able to *calculate* the parameters of the Anderson model. For many Ce compounds, there is a relatively simple relation, within the model, between the most important parameters and experimental data, but this is not generally true. Theoretical information about the parameters is therefore often very helpful. Calculations also reduce the risk that the choice of an oversimplified model, or the use of an inaccurate approxi-

mation in solving the model, is compensated by a choice of unrealistic parameters. The calculation of parameters requires an understanding of the renormalization effects, and comparison with experiment tells us about the quality of our understanding. Finally, the calculation of the parameters represents an important step in the direction of an *ab initio* description of the system.

For the Coulomb integrals $U$ and $U_c$ of the $4f$ and $5f$ metallic systems, Herbst et al.[11] have made important progress. They used the assumption, introduced by Herring for $3d$ systems,[12] that each atom in a solid stays locally neutral, i.e., a change in, e.g., the number of $4f$ electrons is compensated for by a change in the number of conduction electrons so that the net charge of the atomic Wigner-Seitz sphere remains zero. Because of this assumption Herbst et al.[11] could use essentially (renormalized) atomic calculations to obtain renormalized values of $U$ and $U_c$, which implicitly include effects of, for instance, the Coulomb interaction between the $f$ and the conduction electrons. Calculations of this type assume that the conduction electrons adjust instantaneously to the change and the number of localized electrons, and dynamical effects due to the screening by the conduction electrons are neglected. The calculations of Herbst et al.[11] intended for metallic systems, agree well with experimental values for intermetallic Ce compounds.[13,2-4] The renormalization of $U$ and $U_c$ for metallic $f$-electron systems therefore appears to be well understood. For the insulator $CeO_2$ larger values of $U$ and $U_c$ are, however, needed.[14] Similarly, it was found that $U$ is larger for the insulator NiO than for metallic Ni.[9,8] It is therefore interesting to study how a change in the number of localized electrons is screened in nonmetallic systems, to obtain a better understanding of the renormalization of $U$ in such systems. Calculations beyond the renormalized atom approach have been performed by Dederichs et al.,[15] McMahan and Martin,[16] and Wills and Cooper,[17] who performed calculations for solids, but the mechanisms for the screening of a localized electron were not studied explicitly. Here we perform calculations of $U$ and $U_c$ for a Mn impurity in the semiconductor CdTe, to study the screening in detail for a nonmetallic system.

The hopping matrix elements $V$ have also recently been calculated by Sakai et al.,[18] Monnier et al.,[5] McMahan and Martin,[16] Wills and Cooper,[17] and Ehrenreich and co-workers,[19] who used the local-spin-density (LSD) approximation[20] or empirical tight-binding schemes. In this approach it is assumed that the LSD approximation gives a satisfactory description of the many-body effects on the states $|k\sigma\rangle$ and the hopping matrix elements, but that a more careful treatment is required for the many-body effects involving the localized states. In particular, this approach assumes that there are no renormalization effects on $V_{km}$ beyond what is included in the LSD approximation. This approach seems to work well for the cases (spectroscopic[18,16] and magnetic[17] properties of Ce compounds, spectroscopic properties of Yb compounds,[5] and exchange interactions in diluted magnetic semiconductors[19]) where it has been tested, and this suggests that the renormalization of $V$ may be rather small. Some of these calculations[18,5,19] were based on band-structure cal-

culations followed by tight-binding fits to the calculated energy bands. While such a fit can give an excellent description of the energy bands, it is less clear to what extent the individual hopping matrix elements in the fit have a physical meaning. A more satisfactory procedure is to calculate the band structure with the linear muffin-tin orbital (LMTO) method,[21] which is known to give an accurate description of the energy bands in terms of a minimal set of orbitals, and then to use an exact transformation[22] to a set of almost orthogonal, short-ranged LMTO's. Since the states $|k\sigma\rangle$ and $|m\sigma\rangle$ in the Anderson model are normally assumed to be orthogonal, the orthogonality of the LMTO's is convenient. It is furthermore important that a minimal set can be used, because if, as in LCAO-like schemes (where LCAO denotes linear combination of atomic orbitals), more than one orbital for each $lm$ quantum number was used, the identification of a particular orbital with the localized orbital in the Anderson model might be ambiguous. The LMTO method, in the almost orthogonal representation, provides a direct mapping onto the Anderson Hamiltonian. McMahan and Martin[16] used the almost orthogonal LMTO's to calculate the hopping matrix elements $V_{km}$ as a sum over matrix elements of the LMTO Hamiltonian times the eigenvector of the state $|k\sigma\rangle$. Wills and Cooper[17] used the original nonorthogonal LMTO orbitals and expressed $V_{km}$ in terms of eigenvector for the state $|k\sigma\rangle$, structure constants, and a potential parameter. Here we shall follow a different route.

In the Anderson impurity model the individual hopping matrix elements are not needed, but just a particular combination. To see this[2] we write the coupling term in (1) as

$$\sum_{m,\sigma} \left[ \psi_{m\sigma}^{\dagger} \int d\varepsilon\, V_m(\varepsilon)\psi_{\varepsilon m\sigma} + \text{H.c.} \right] \tag{2}$$

using the linear combination

$$|\varepsilon m\sigma\rangle = \frac{1}{V_m(\varepsilon)} \sum_k V_{km}\delta(\varepsilon-\varepsilon_{k\sigma})|k\sigma\rangle , \tag{3}$$

of extended states, where $V_m(\varepsilon)$ is defined below. These states are orthogonal if[2]

$$\sum_k V_{km}^* V_{km}\cdot\delta(\varepsilon-\varepsilon_k) = |V_m(\varepsilon)|^2 \delta_{mm'} \equiv \frac{1}{\pi}\Delta_m(\varepsilon)\delta_{mm'} , \tag{4}$$

which is fulfilled if $m$ and $m'$ label different irreducible representations or different partners of the same representation of the point group of the impurity site.[23] The remaining extended states are chosen to be orthogonal to (3) and it is easy to show that they do not couple to the localized states. The Hamiltonian (1) then takes the form

$$H = \sum_{\nu} \left[ \int \varepsilon\psi_{\varepsilon\nu}^{\dagger}\psi_{\varepsilon\nu}d\varepsilon + \varepsilon_\nu\psi_\nu^{\dagger}\psi_\nu \right.$$
$$\left. + \int [V_\nu(\varepsilon)\psi_\nu^{\dagger}\psi_{\varepsilon\nu} + \text{H.c.}]d\varepsilon \right]$$
$$+ U\sum_{\substack{\nu,\mu \\ \nu<\mu}} n_\nu n_\mu + H_0 , \tag{5}$$

where $v=(m,\sigma)$ and $H_0$ contains the extended states which do not couple to the localized states. It is now clear that the coupling between the localized states and the extended states is entirely described by the quantity $\Delta_v(\varepsilon)$, which has the dimension energy. Due to the definition (3), the density of new states $|\varepsilon v\rangle$ is unity inside the band. It should be observed that $\Delta_m(\varepsilon)$ in (4) does not contain enough information about the hopping matrix elements to obtain the solution of the *periodic* Anderson model.

We can now ask for the diagonal matrix element of the one-particle Green's function for a localized state $|v\rangle$. In the limit of $U=0$, standard calculations (Löwdin partitioning) give[1]

$$G_{vv}(z)\equiv\left\langle v\left|\frac{1}{z-H}\right|v\right\rangle=\frac{1}{z-\varepsilon_v-\Gamma_v(z)}\ ,\qquad(6)$$

where

$$\Gamma_v(z)=\sum_k\frac{V_{km}^*V_{km}}{z-\varepsilon_k}=\int d\varepsilon\frac{|V_v(\varepsilon)|^2}{z-\varepsilon}\ .\qquad(7)$$

It then follows that

$$\pi|V_v(\varepsilon)|^2\equiv\Delta_v(\varepsilon)$$
$$=-\mathrm{Im}\left[\frac{1}{G_{vv}(\varepsilon-i0)}\right]$$
$$=-\mathrm{Im}\left[\left[\int d\varepsilon'\frac{\rho_v(\varepsilon')}{\varepsilon-\varepsilon'-i0}\right]^{-1}\right]\ ,\qquad(8)$$

where $\rho_v$ is the density of states for $H$ (in the limit $U=0$) projected onto the localized orbital. The steps (6)–(8) can be performed formally also within the local-density (LD) approximation giving the same final result (8). We can therefore calculate $\rho_v^{\mathrm{LD}}(\varepsilon)$, using the methods described below, and then deduce the LD result for $\Delta_v(\varepsilon)$ from Eq. (8). Equation (8) is therefore a key result. The result (8) has *not* been obtained by perturbation theory, but is valid for any strength of the hopping matrix elements. In Sec. III we calculate $\rho_v(\varepsilon)$ using the atomic-sphere approximation (ASA) for the one-electron potential, but from the derivation of (8) it is clear that this result is also valid if $\rho_v(\varepsilon)$ is calculated for the full potential. Below, (8) is applied to semiconductors, but exactly the same technique can be used for metals.

By expressing $\Delta_v(\varepsilon)$ in terms of the local density of states, we have obtained a rather "representation-independent" expression. Assuming that the calculation of the Green's function is accurate, the result depends only on how the localized orbital $|v\rangle$ is defined, not on how the other orbitals are defined. In particular, the issue of the orthogonality of the localized states $|m\sigma\rangle$ to the other states used in the calculations of $\rho_v^{\mathrm{LD}}(\varepsilon)$ is not raised in this formulation.

The Anderson impurity model has been used both for a chemical impurity in some host and for a periodic system. In the latter case one ought to use the periodic Anderson model, with the Coulomb interaction on all the sites of the lattice. Because of the difficulty of finding an accurate solution for the periodic Anderson model, the Anderson impurity model is, however, often used for the periodic case, too. In terms of the type of system discussed here, $Cd_{1-x}Mn_xTe$, we can thus either treat one Mn atom replacing a Cd atom in CdTe (i.e., the $x=0$ limit), or we can consider the periodic arrangement MnTe (the $x=1$ limit). In the calculations to be reported in the following we have studied the first case.

When the Anderson impurity model is used to describe a chemical $(x\rightarrow0)$ impurity, the Green's function in (8) refers to the Green's function of the impurity system, which can be obtained by solving the Dyson's equation. If the perturbation due to the impurity is limited to the impurity atom, i.e., the potential of the atoms surrounding the impurity is unchanged, Dyson's equation blocks into small submatrices. $\Delta_v(\varepsilon)$ is then obtained from the unperturbed Green's function and the potential on the impurity site via the inversion of a matrix, which with a basis of LMTO's and in the ASA is only $1\times1$ or $2\times2$. For the case considered here, Mn in CdTe, it is then sufficient to know the potential of the Mn atom and the on-site Green's function of CdTe, which can be obtained from a Hilbert transform of the Cd $3d$ ($E$) or $3d$ ($T_2$) projected densities of states for the unperturbed CdTe crystal.

When the Anderson impurity model is used to describe a periodic system, the Green's function in (8) refers to the periodic system. The matrix element needed in (8) is then simply obtained from the projected density of states of a band calculation for a periodic system, and there is no Dyson equation to be solved. In this approach some aspects of the periodicity of the system are included in the Anderson impurity model. In particular, for $U=0$ the *impurity* model reproduces exactly the density of states projected onto the localized orbital for the *periodic* system. For large values of $U$, further study is needed to determine whether or not the description of the system is improved when the localized orbital on the other sites are included in the LSD calculation of the hopping matrix elements used in the impurity model. It is important to note that in the definition of "extended" states $|k\sigma\rangle$ in (1), we have excluded the localized orbitals on the impurity site because these are treated *explicitly*. The spectrum $\varepsilon_k$ for, e.g., MnTe is therefore obtained with the $3d$ orbitals on one Mn atom removed. The removal of the localized orbital from the crystal can in some cases lead to "dangling bonds" and associated bound states. The relation between the density of states of MnTe and the $\varepsilon_k$ in (1) is therefore not necessarily trivial.

Normally the same hopping matrix elements are used in the Anderson model both in the presence and the absence of a core hole, although it is clear that the core hole will have an influence on the hopping matrix elements.[24,25,8] In particular, Zaanen and Sawatzky[8] observed that for NiO the spectra would be better described if it were assumed that the presence of a core hole increases the hopping matrix elements. This raises the question of how strongly $\Delta_v(\varepsilon)$ is influenced by a core hole, and in which direction the change goes. Since the hopping matrix element

$$V_{kv}\equiv\langle k|H|v\rangle\qquad(9)$$

is a matrix element of the Hamiltonian, which includes the potential, one may argue that the attractive core-hole potential should increase the strength $|V|$ of the hybridization. On the other hand, the attractive potential makes the localized state $|v\rangle$ even more localized and reduces the overlap to the extended states $|k\rangle$. One may therefore also argue that $|V|$ is reduced. We have performed calculations for Mn in CdTe to determine which effect dominates.

In Sec. II we present the formalism for calculating the hybridization $\Delta_v(\varepsilon)$ within the LMTO formalism and in Sec. III we present the results. The calculations of $U$ and $U_c$ are described in Secs. IV and V, respectively. In Sec. VI we present a preliminary calculation of the photoemission spectrum, and we make some concluding remarks in Sec. VII. A preliminary account of this work has been presented in a conference proceedings.[26]

## II. CALCULATION OF HOPPING MATRIX ELEMENTS IN THE LMTO FORMALISM

Below we describe how the LMTO-ASA formalism[21,22] can be used to calculate the quantity $\Delta_v(\varepsilon)$, which contains the information about the hopping matrix elements needed in the Anderson model. In the ASA the one-electron potential is spherical inside the Wigner-Seitz spheres centered at the atoms, and in open structures, at interstitial sites. The ASA usually gives hopping integrals accurate to a few percent.[27] The LMTO's defined below form a complete basis for the ASA potential, and a highly accurate basis for the full potential, as recently demonstrated.[28]

We thus assume that space is divided into slightly overlapping Wigner-Seitz spheres, which together have the same volume as the crystal. The interstitial volume between the spheres is neglected, and for simplicity we assume that all spheres have the same Wigner-Seitz radius $s$. The traditional LMTO's (Ref. 21) are expressed in terms of an envelope function, $K^0$, which is the irregular solution to the Laplace equation corresponding to the angular momentum $L = (l, m)$ centered on the sphere at $\mathbf{R}$. It decays as $r^{-l-1}$. In all the other spheres, this function may be expanded in terms of the regular solutions $J^0 \sim r^l$ of the Laplace equation. The one-center expansions of the envelope function may thus be expressed as

$$|K^0\rangle^\infty = |K^0\rangle - |J^0\rangle S^0 ,\tag{10}$$

where the superscript $\infty$ indicates a function extending over all space and the absence of this superscript implies a function truncated outside the sphere on which it is centered. In Eq. (10), $S^0$ is the conventional structure matrix $S_{\mathbf{R}'L',\mathbf{R}L}$ and a summation over $\mathbf{R}'$ and $L'$ is implied. This envelope function is augmented analogously to the way described below to obtain muffin-tin orbitals. These orbitals are long ranged and nonorthogonal, which makes them less suitable for our purposes. We use instead a recent version of the LMTO formalism[22] which allows the construction of short-ranged almost orthogonal orbitals. These are obtained by forming linear combinations of the envelope functions (10) in such a way that the orbitals obtain the desired properties. For this

purpose we introduce the function

$$|J^\alpha\rangle = |J^0\rangle - |K^0\rangle\alpha ,\tag{11}$$

where $\alpha_{\mathbf{R}l}$ are so-called screening parameters which specify the LMTO representation and which will be chosen later. The new envelope has the one-center expansion

$$|K^\alpha\rangle^\infty = |K^0\rangle - |J^\alpha\rangle S^\alpha .\tag{12}$$

By requiring that this function is a linear combination of the functions (10), one finds that the new structure matrix is related to the conventional one through

$$(S^\alpha)^{-1} = (S^0)^{-1} - \alpha .\tag{13}$$

Here $\alpha$ is to be regarded as a diagonal matrix, and the structure matrix is Hermitian. Whereas the one-site terms of $S^0$ vanish, this is generally not the case for $S^\alpha$.

To augment the envelope function, we introduce a normalized solution $\phi_{\mathbf{R}L}(\varepsilon, \mathbf{r})$ of the Schrödinger equation inside the sphere at $\mathbf{R}$. The function $K^0$ in (12) is now replaced by[22]

$$K^0(\mathbf{r}) \rightarrow \phi(\varepsilon, \mathbf{r})N^\alpha(\varepsilon) + \tilde{J}^\alpha(\mathbf{r})P^\alpha(\varepsilon) ,\tag{14}$$

where $\tilde{J}^\alpha$ is a function which matches continuously and differentiably onto $J^\alpha$ at the sphere surface. The functions $N^\alpha$ and $P^\alpha$ are chosen so that the right-hand side of (14) matches continuously and differentiably onto $K^0$ at the sphere surface. This gives[22]

$$N^\alpha(\varepsilon) = \left[\frac{s}{2}\dot{P}^\alpha(\varepsilon)\right]^{1/2} ,\tag{15}$$

where $\dot{P}^\alpha(\varepsilon)$ is the energy derivative of $P^\alpha(\varepsilon)$ and

$$[P^\alpha(\varepsilon)]^{-1} + \alpha = [P^0(\varepsilon)]^{-1} = \frac{1}{2(2l+1)}\frac{D(\varepsilon)-l}{D(\varepsilon)+l+1}\tag{16}$$

is expressed in terms of the logarithmic derivative $D(\varepsilon)$ of the radial Schrödinger equation solution. An energy-dependent muffin-tin orbital $|\chi^\alpha(\varepsilon)\rangle^\infty$ is now defined by replacing $J^\alpha$ by $\tilde{J}^\alpha$ in the envelope function (12) as well. Using (14) one obtains[22]

$$|\chi^\alpha(\varepsilon)\rangle^\infty = |\phi(\varepsilon)\rangle N^\alpha(\varepsilon) + |\tilde{J}^\alpha\rangle[P^\alpha(\varepsilon) - S^\alpha] .\tag{17}$$

This function is a linear combination of $|\phi(\varepsilon)\rangle$ and $|\tilde{J}^\alpha\rangle$ in the sphere at which it is centered, and in all other spheres it is defined in terms of $|\tilde{J}^\alpha\rangle$.

An energy-independent (linear) muffin-tin orbital (LMTO) is introduced by fixing $\varepsilon = \tilde{\varepsilon}$, where $\tilde{\varepsilon}$ is an arbitrary energy chosen in the energy range of interest. It is further required that $|\tilde{J}^\alpha\rangle$ is chosen so that the energy derivative of $|\chi(\varepsilon)\rangle^\infty$ is zero at $\varepsilon = \tilde{\varepsilon}$.[22] Then

$$|\tilde{J}^\alpha\rangle = -|\dot{\phi}^\alpha\rangle\frac{s}{2N^\alpha} ,\tag{18}$$

where

$$|\dot{\phi}^\alpha\rangle = |\dot{\phi}^\gamma\rangle + |\phi\rangle o^\alpha .\tag{19}$$

Here $|\dot{\phi}^\gamma\rangle$ is the energy derivative of the solution $|\phi(\varepsilon)\rangle$

normalized to unity in the sphere, and

$$o^{\alpha} = \dot{N}^{\alpha}/N^{\alpha} \ . \tag{20}$$

Here and in the following an omitted energy argument indicates that $\varepsilon = \bar{\varepsilon}$. The LMTO is finally defined as

$$|\chi^{\alpha}\rangle^{\infty} \equiv |\chi^{\alpha}(\bar{\varepsilon})\rangle^{\infty} \frac{1}{N^{\alpha}} \equiv |\phi\rangle + |\dot{\phi}^{\alpha}\rangle h^{\alpha} \ , \tag{21}$$

where

$$h^{\alpha} = -\frac{1}{(\dot{P}^{\alpha})^{1/2}}(P^{\alpha} - S^{\alpha})\frac{1}{(\dot{P}^{\alpha})^{1/2}} \ . \tag{22}$$

In the ASA it is now possible to express the overlap $O$ and Hamiltonian $H$ matrix elements between the LMTO's in terms of the $h^{\alpha}$ and $o^{\alpha}$ as[22]

$$O^{\alpha} = (1 + h^{\alpha}o^{\alpha})(o^{\alpha}h^{\alpha} + 1) + h^{\alpha}ph^{\alpha} \tag{23}$$

and

$$H^{\alpha} = h^{\alpha}(1 + o^{\alpha}h^{\alpha}) + (1 + h^{\alpha}o^{\alpha})\bar{\varepsilon}(o^{\alpha}h^{\alpha} + 1) + h^{\alpha}\bar{\varepsilon}ph^{\alpha} \ , \tag{24}$$

where

$$p = \langle(\dot{\phi}^{\gamma})^2\rangle \tag{25}$$

is the integral of $(\dot{\phi}^{\gamma})^2$ in its sphere. In the above matrix equations all matrices except $S^{\alpha}$ and $h^{\alpha}$ are diagonal.

The inverse of the potential function, $1/P^{\alpha}(\varepsilon)$, is essentially minus tangent of the phase shift, and it may be parametrized by the usual resonance form[22]

$$\frac{1}{P^{\alpha}(\varepsilon)} = \frac{\tilde{\Delta}}{\varepsilon - C} + \gamma - \alpha \ . \tag{26}$$

Thus the system is characterized by the structure constants $S^{\alpha}$ and the potential parameters $C$, $\tilde{\Delta}$, $\gamma$, and $p$, where $C$ determines the center of a resonance and $\tilde{\Delta}$ its width.

The nearly orthogonal representation is finally obtained by setting the free parameters $\alpha_{Rl}$ equal to the parameters $\gamma_{Rl}$, determined by the potential according to (26). Then the potential functions are linear and $o^{\alpha}$, defined in (20), vanishes. In this representation the overlap matrix

$$O^{\gamma} = 1 + h^{\gamma}ph^{\gamma} \tag{27}$$

is then the unit matrix, apart from the term $h^{\gamma}ph^{\gamma}$, which is normally small. Thus the choice of $\alpha = \gamma$ leads to approximately orthogonal orbitals.[22] Neglecting the term proportional to $h^{\gamma}ph^{\gamma}$ also in $H^{\gamma}$, we obtain using (22), (24), and (26) with $\alpha \equiv \gamma$,

$$H^{\gamma} = \bar{\varepsilon} + h^{\gamma} = C + \tilde{\Delta}^{1/2}S^{\gamma}\tilde{\Delta}^{1/2} \ . \tag{28}$$

Note that the hopping integral from orbital $RL$ to $R'L'$ is proportional to the square root of $\tilde{\Delta}_{RL}\tilde{\Delta}_{R'L'}$. Below (Table I) we show for $Cd_{1-x}Mn_xTe$ that the nearly orthogonal orbitals are relatively short ranged.

We now introduce the Green's function[29]

$$G(z) = (z - H^{\gamma})^{-1} \ . \tag{29}$$

The matrix element $G_{vv}$ is identified with the corresponding matrix element of the $U = 0$ Green's function of the Anderson model, and the value of $\Delta_v(\varepsilon)$ is determined as discussed in the Introduction. For substitutional Mn in CdTe we have to calculate $G$ of an impurity system. The solution of the corresponding Dyson equation is greatly simplified if we consider the related Green's function[29]

$$g^{\alpha}(z) = [P^{\alpha}(z) - S^{\alpha}]^{-1'} \ . \tag{30}$$

This Green's function satisfies a Dyson equation

$$(g^{\alpha})^{-1} = (g_0^{\alpha})^{-1} + (P^{\alpha} - P_0^{\alpha}) \ , \tag{31}$$

whose perturbation $P^{\alpha} - P_0^{\alpha}$ is localized to the spheres where the potential is changed, while the corresponding Dyson equation for $G$ has a nonzero perturbation for all orbitals with tails extending into the perturbed region. In Eq. (31), $g^{\alpha}$ and $g_0^{\alpha}$ are the Green's functions with and without the impurity, respectively. The relation between $G$ and $g^{\gamma}$ is[29]

$$g^{\gamma}(z) = \tilde{\Delta}^{1/2}G(z)\tilde{\Delta}^{1/2} \tag{32}$$

as seen from (28)–(30) and (26). The relation between $g^{\alpha}$ and $g^{\gamma}$ is shown in Ref. 22 to be

$$g^{\alpha}(z) = \frac{P^{\gamma}(z)}{P^{\alpha}(z)}g^{\gamma}(z)\frac{P^{\gamma}(z)}{P^{\alpha}(z)} - (\gamma - \alpha)\frac{P^{\gamma}(z)}{P^{\alpha}(z)} \ . \tag{33}$$

To obtain $\Delta_v(\varepsilon)$ we first calculate $G_0(z)$ for the host crystal (e.g., CdTe) using (28) and (29) with potential parameters $C_0$, $\tilde{\Delta}_0$, and $\gamma_0$, corresponding to the host potential. Then the $\gamma$ values for the perturbed potential are calculated, and $g_0^{\gamma_0}(z)$ is transformed to the $\gamma$ representation using Eq. (33) with $\alpha \to \gamma$ and $\gamma \to \gamma_0$. Then the Dyson equation (31) is solved, and we transform back to $G$ using (32). Finally, $\Delta_v(\varepsilon)$ is obtained from (8). As a result,

$$\Delta_v(\varepsilon) = -\tilde{\Delta}_v \text{Im}\left[\frac{1}{g_{vv}^{\gamma}(\varepsilon - i0)}\right] \ . \tag{34}$$

For the cases we have tried, it is sufficient to solve the Dyson equation assuming that the perturbation is limited to the impurity atom, since the hopping matrix elements are not very sensitive to the moderate changes in the potential which result from assuming a larger perturbed region. In the case of a Mn impurity substituting a Cd atom in CdTe, this means that we only need to deal with matrices of, at most, the size $2 \times 2$: for the $T_2$ symmetry the perturbation on Mn mixes states of $4p$ and $3d$ character. If however, we assume that the potential function is the same for the Cd and Mn $p$ electrons, the Dyson equation is reduced to a $1 \times 1$ matrix. Since $P$ is real, it follows from (31) that for the $1 \times 1$ case, $\text{Im}g_{vv}^{-1}$ is unchanged by the perturbation, and we have

$$\Delta_v(\varepsilon) = -\tilde{\Delta}_v \text{Im}\left[\frac{1}{g_{0vv}^{\gamma}(\varepsilon - i0)}\right] \ . \tag{35}$$

The "on-site" Green's function $g_{0vv}^{\gamma}$ can be obtained from

a Hilbert transform of the appropriate projected density of states $\rho_{0v}$ of the unperturbed host. This leads to

$$\Delta_v(\varepsilon) = -\frac{\bar{\Delta}_v}{\bar{\Delta}_0}\text{Im}\left[\left[\int d\varepsilon' \frac{\rho_{0v}(\varepsilon')}{\varepsilon - \varepsilon' - i0}\right]^{-1}\right], \qquad (36)$$

where $\bar{\Delta}_0$ refers to the unperturbed host. In the next section we demonstrate that this formula is sufficiently accurate for Mn in CdTe.

In order to discuss the dependence of $\Delta_v(\varepsilon)$ in (35) on the potential parameters, we use Löwdin partitioning as in (6), but for $[(P-S)^{-1}]_{vv}$ rather than for $[(z-H)^{-1}]_{vv}$. The resulting expression is

$$-\text{Im}\left[\frac{1}{g^\gamma_{0vv}(\varepsilon - i0)}\right]$$

$$= \text{Im}(S^\gamma_{vn}\{[P^\gamma(\varepsilon - i0) - S^\gamma]_{nn}\}^{-1}S^\gamma_{nv}), \qquad (37)$$

where $n = (\mathbf{R}L)$ labels all sites and angular momenta *other* than those of the impurity orbital. Hence, $S_{vn}$ is a rectangular matrix of size $1 \times (N-1)$ and $S_{nn}$ is a square matrix of size $(N-1) \times (N-1)$, with $N$ being the total number of orbitals in the solid. An alternative way of obtaining (35) and (37) is to use the definition (4) of $\Delta_v(\varepsilon)$ together with (9), (28), and (26) with $\alpha = \gamma$. It is now obvious, first of all that $\Delta_v(\varepsilon)$ is *independent* of the potential parameters $C_{0v}$, $\bar{\Delta}_{0v}$, and $\gamma_{0v}$ for the host orbital which is substituted by the impurity orbital. More importantly, $\Delta_v(\varepsilon)$ is *independent of the position*, $C_v$, and *proportional to the width*, $\bar{\Delta}_v$, of the impurity resonance. Note that $\bar{\Delta}_v$ gives the squared amplitude of the impurity orbital tail [see (21) and (28)]. The only remaining dependence of the hybridization function on the impurity-potential parameters is the $\gamma_v$ dependence via the structure matrix in (37). The shape of the impurity orbital is weakly influenced by $\gamma_v$. The dependence of $\Delta_v(\varepsilon)$ is implicit because, in principle, all the elements of the structure matrix depend on $\gamma_v$. For a first-order change in $\gamma_v$, we find from (13) that

$$\frac{\partial S^\gamma_{\mathbf{R}L,\mathbf{R}'L'}}{\partial \gamma_v} = S^\gamma_{\mathbf{R}L,v}S^\gamma_{v,\mathbf{R}'L'}, \qquad (38)$$

and using this in (37) yields the result

$$\frac{1}{2\Delta_v(\varepsilon)}\frac{\partial \Delta_v(\varepsilon)}{\partial \gamma_v}$$

$$= S^\gamma_{vv} + \text{Re}(S^\gamma_{vn}\{[P^\gamma(\varepsilon) - S^\gamma]_{nn}\}^{-1}S^\gamma_{nv}). \qquad (39)$$

Typical values for the on-site elements, $S^\gamma_{dd}$, are between 1 and 7, and $\gamma_d$ values for $3d$ transition elements lie between $-0.01$ and $0.01$. If we therefore take $\partial \gamma_v = 0.01$, the first energy-independent term of (39) yields merely a 2–14% change of $\Delta_v(\varepsilon)$. Full calculations for Mn in CdTe show that within the valence band and within the conduction band up to 5 eV above the bottom of the band, $\Delta_v(\varepsilon)$ changes by less than about 10% for $\partial \gamma_{\text{Mn}\,d} = 0.01$. This weak dependence of $\Delta_v(\varepsilon)$ on $\gamma_v$ is connected with the fact that the impurity orbital, $|\chi^\gamma_v\rangle$ in (21), depends weakly on $\gamma_v$. The reason is that all the functions $|\dot{\phi}^{\gamma_n}_n\rangle$ augmenting the tail are independent of

$\gamma_v$, and the function $|\phi_v\rangle + |\dot{\phi}^{\gamma_v}_v\rangle h^\gamma_{vv}$ augmenting the head has a logarithmic derivative at the impurity sphere which is independent of $\gamma_v$ to first order, as may easily be proved using (12) and (38) with $\mathbf{R}L = \mathbf{R}'L' = v$. Since the LMTO is everywhere continuous and differentiable, it can only depend weakly on the $\gamma$ value in its own sphere. This explains why we find that $\Delta_v(\varepsilon)$ primarily depends only on $\bar{\Delta}_v$ and the host properties.

## III. RESULTS FOR THE HOPPING MATRIX ELEMENTS OF Mn IN CdTe

We have performed LSD calculations for Mn impurities in CdTe using the LMTO-ASA formalism developed earlier.[29] As usual, empty spheres are introduced in the large interstitial spaces of this system. The unit cell of CdTe therefore contains a Cd, a Te, and two empty spheres. In this way the radius ($s = 3.015$ a.u.) of the spheres can be chosen so that the spheres are space filling, without having a large overlap. The potential inside each sphere was assumed to be spherically symmetric (ASA), and a frozen-core approximation was used. The basis set consisted of the nine $s$, $p$, and $d$ LMTO's centered at the atomic and at the empty sites. As discussed in Sec. II, the free parameter $\alpha$ can be used to define orbitals with different properties. Here we use $\alpha = \gamma$, where $\gamma$ is a parameter determined by the potential, to obtain approximately orthogonal orbitals.[22] To compensate for the well-known problem that the LSD approximation gives a too small gap for semiconductors,[30] the so-called scissor operator was used.[31] We have assumed that the atoms surrounding the Mn atom do not relax their positions, relative to the unperturbed CdTe lattice. Since we expect the hopping matrix elements to depend rather sensitively on the atomic distances, the relaxation should be studied further. As indicated below (31), it is convenient to solve the problem by using the Green's function $g$ defined in (30). The solution of the Dyson equation then involves a matrix problem, where the matrix size is determined by the number of orbitals centered on sites where the potential is perturbed by the impurity. This is in contrast to LCAO schemes, where we have to include all orbitals with tails extending into the perturbed region. For this reason it is sufficient to include only the orbitals centered on the Mn atom and the nearest-neighbor Te and empty sites. Even the inclusion of just the Mn orbitals is a fairly good approximation. The calculations show that there are about 5.4 $3d$ electrons in the Mn sphere, with a large magnetic moment of about $4.4\mu_B$.

We first consider the results for the LMTO's defined in the preceding section, to determine to what extent the nearly orthogonal $3d$ orbitals are appropriate to use in the definition (6) of the Green's function $G_{vv}$, which determines the hybridization $\Delta v(\varepsilon)$. In particular, we would like the Mn $3d$ orbital to be short ranged and mainly localized inside the Mn sphere. Table I shows how the contributions to the overlap integral of a $3d$ orbital with itself are distributed between spheres at different distances from the site where the orbital is centered. The orbitals are seen to be reasonably short

TABLE I. The contributions to the overlap integral of a Mn $3d$ orbital with itself from the spheres at a given distance from the central sphere. Results are shown for orbitals of $E$ and $T_2$ symmetry. The distances are given in units of the Wigner-Seitz radius.

| Distance | $E$ | $T_2$ |
|----------|-----|-------|
| 0.0 | 1.000 041 | 1.0033 |
| 1.7589 | 0.000 35 | 0.0040 |
| 2.0310 | 0.000 27 | 0.000 030 |
| 2.8722 | 0.000 018 | 0.000 190 |
| 3.3673 | 0.000 022 | 0.000 009 |
| 3.5178 | 0.000 004 | 0.000 100 |
| 4.0620 | 0.000 004 | 0.000 000 |
| 4.4260 | 0.000 000 | 0.000 000 |

ranged and almost all the weight is concentrated inside the Mn sphere. We therefore believe that these orbitals are well suited to represent the localized orbitals in the Anderson model.

The hybridization $\Delta_v(\varepsilon)$ [see (4) and (5)] is now calculated using (34) and the almost orthogonal orbitals. Because of the spin polarization, the results are different for spin up and spin down. Figure 1 shows the average of the spin-up and spin-down results for the $E$ and $T_2$ symmetries. The curves in the top part of the figure were obtained by calculating the perturbed Green's function $g$, assuming that the region perturbed by the Mn atom consists of the nearest-neighbor Te and empty spheres. The middle part of the figure shows results obtained by as-
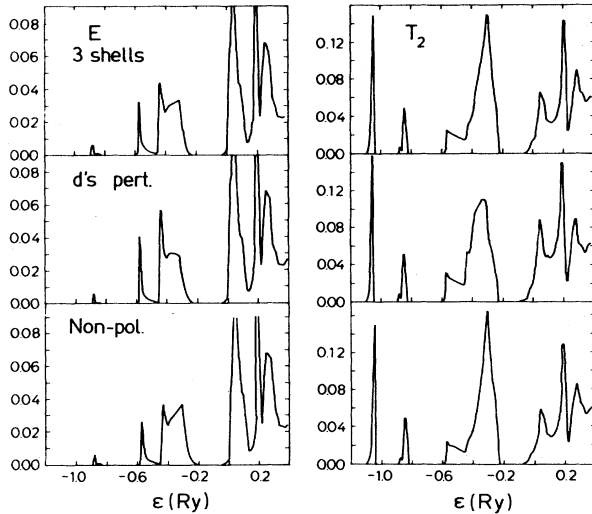


FIG. 1. The coupling $\Delta_v(\varepsilon)$ for the $E$ and $T_2$ symmetries. The top part shows the result of solving Dyson's equation for the perturbed region (one Mn atom, four Te atoms, and four empty sites) and the middle part the result of only considering the $1 \times 1$ matrix corresponding to a $3d$ state. Both the top and middle part show averages of spin-up and spin-down results. The lower part shows results from a nonpolarized calculation, using the same perturbed region as in the top part of the figure. These calculations were performed for the ground-state $3d$ occupancy. The energy unit is Ry.

suming that only the $d$ orbital is perturbed when Cd is replaced by Mn. In the latter case the solution of the Dyson equation only involves $1 \times 1$ matrices, as discussed at the end of Sec. II. The results are quite similar. At $\varepsilon = -1.05$ Ry there is a peak in the $T_2$ function, which is due to the Te $5s$ band. For symmetry reasons there is no contribution of the Te $5s$ states to states of $E$ symmetry. At about $\varepsilon = -0.85$ Ry there is another peak corresponding to the Cd $4d$ band. This peak has relatively little weight, since the Mn atom has no Cd nearest neighbor. The weight in the range $-0.6$ to $-0.2$ Ry corresponds to the coupling to the valence band. This band has in particular Te $5p$ character, but many other types of states also have a substantial weight. The contribution above $-0.1$ Ry is due to the coupling to the conduction band. The integrated value of $\Delta_v(\varepsilon)$ over the valence band is about 3.2 (spin up) and 3.3 (spin down) times larger for the $T_2$ symmetry than for the $E$ symmetry. As a check of these results we have used Harrison's semiempirical tight-binding scheme[32] to calculate the ratio of the $T_2$ to $E$ coupling. The valence band was for simplicity assumed to have only Te $5p$ character, and Harrison's ratio 2.17 between the $V_{pd\sigma}$ and $V_{pd\pi}$ was used, where $V_{pd\sigma}$ and $V_{pd\pi}$ refer to the $pd$ hopping matrix elements of $\sigma$ and $\pi$ character, respectively. This leads to a ratio of 2.7 for the $T_2$ to $E$ coupling, which is fairly close to our calculated value. In Harrison's scheme the integrated strength is 0.0023 $Ry^2$ for the $E$ symmetry, which is about 0.4 of our calculated values of 0.0051 (spin up) and 0.0067 (spin down) $Ry^2$.

Figure 1 shows that the coupling to the conduction band is fairly strong. In a very simple picture one may associate the valence band with the Te $5p$ and the conduction band with Cd $5s$ states. If this were correct, the coupling to the conduction states would be very weak, since the Mn $3d$ could then only couple to the conduction band via hopping to the second-nearest neighbors. The figure illustrates that such a picture is oversimplified.

The Anderson model is invariant under rotations in spin space, and the hopping matrix elements are independent of the spin index. Because of the large magnetic momentum $(4.4\mu_B)$ in the LSD calculation, there is, however, a substantial spin dependence of the calculated matrix elements. This suggests the use of the average of the spin-up and spin-down results, or the use of results obtained from a nonpolarized calculation. These results are compared in the top and bottom parts of Fig. 1. To obtain a neutral solution in the nonpolarized calculation, bound levels must be occupied. We have considered the state where the $T_2$ level is fivefold occupied. The $3d$ charge inside the Mn sphere is 5.5, which is rather close to the result (5.4) for the spin-polarized solution. The figure shows that the averaged spin-polarized result and the nonpolarized result are rather similar. For the nonpolarized curves there is a certain shift of weight towards the top of the valence band, while the overall weight is similar for the two cases. This is also illustrated by the fact that $\bar{\Delta}$ is 0.0098 Ry in the nonpolarized calculation and the average of the spin-up and spin-down $\bar{\Delta}$ is 0.0100 Ry in the spin-polarized calculation.

The calculations above were performed for the

ground-state charge density of Mn in CdTe. It is in-
teresting to ask how $\Delta_v(\varepsilon)$ changes when the Mn
configuration changes, since the configurations of impor-
tance depend on the experiment or property studied.
From (35) it follows that we only need the host Green's
function $g^\gamma_{0vv}$ and the potential parameter $\tilde{\Delta}_v$ for the cal-
culation of $\Delta_v(\varepsilon)$. Since this Green's function depends on
the impurity potential only via the potential parameter $\gamma$,
and since this dependence is very weak, we focus on the
dependence of $\tilde{\Delta}_v$ on the configuration. We can therefore
break the coupling of the Mn $3d$ orbital to the rest of the
orbitals and force it to have the occupancy of interest.
We then calculate the corresponding Mn potential and $3d$
wave function, allowing the system to relax, for instance
via a charge transfer to the Mn $4s$ and $4p$ orbitals. The
results for $\tilde{\Delta}_{3d}$ are shown in Table II, which illustrates
that there is a substantial variation with the net charge
on the Mn atom.

We discussed in the Introduction how in a LCAO pic-
ture one may argue about whether the introduction of a
core hole would increase or decrease the hopping matrix
elements, since in this picture one can think of the core
hole as having two opposing effects on the matrix ele-
ments. The present calculations show that the net effect
is a reduction of the matrix elements. In the LMTO for-
malism this is rather straightforward to see, since in this
case $\Delta_v(\varepsilon)$ scales with $\tilde{\Delta}_v$. This quantity is given by[21,22]

$$\tilde{\Delta} \approx \frac{s}{2}[\phi(C,s)]^2 , \qquad (40)$$

where $\phi(C,s)$ is the value at the Wigner-Seitz radius $s$ of
the normalized solution of the radial Schrödinger equa-
tion calculated at the energy $C$, the position of the reso-
nance, which corresponds to the boundary condition that
the logarithmic derivative at $s$ is $-l-1$. When the po-
tential is made more attractive, the orbital contracts and
its value at the Wigner-Seitz sphere is reduced, leading to
a reduction in the value of $\tilde{\Delta}$.

The large variation of $\tilde{\Delta}_{3d}$ with the Mn configuration
shows that the Anderson model should be used with
some caution, and it suggests that the apparent value of
$\Delta_v(\varepsilon)$ may be different for different experiments. This
effect is, however, counteracted by the tendency of the
system to stay neutral. In core-level spectroscopy, for in-
stance, the core hole is for many systems screened by a
localized electron. It is therefore interesting to compare
$\tilde{\Delta}_{3d}$ calculated for $n_c = 2$ and $n_d = 5$ with the value calcu-
lated for $n_c = 1$ and $n_d = 6$. From Table II we find that in
this case the change of $\tilde{\Delta}_{3d}$ is only about 20%.

TABLE II. The potential parameter $\tilde{\Delta}_{3d}$ for different Mn
configurations in a non-spin-polarized calculation. The energy
unit is Ry.

| $n_d$ | $n_{1s}$ | $\tilde{\Delta}_{3d}$ |
|---|---|---|
| 4 | 2 | 0.0051 |
| 5 | 2 | 0.0085 |
| 6 | 2 | 0.0129 |
| 5 | 1 | 0.0040 |
| 6 | 1 | 0.0067 |

TABLE III. The induced charge on the central Mn site, par-
titioned in $l$ components, and on the four Te and empty sites,
when a Mn $1s$ hole is created.

| Mn $4s$ | Mn $4p$ | Mn $3d$ | Te | Empty |
|---|---|---|---|---|
| −0.002 | −0.009 | 1.126 | −0.087 | −0.029 |

To illustrate this point further we have performed self-
consistent calculations, including the coupling to the Mn
$3d$ orbital again, for a $1s$ core hole in Mn. We have con-
sidered a neutral state, where one of the spin-down bound
states in the energy gap of $E$ symmetry has been occu-
pied. A state with a positive charge, i.e., with all bound
spin-down levels unoccupied, does not exist. Table III
shows the change in the charge density when the core
hole is created. The hole is somewhat overscreened, since
the charge in the Mn sphere increases by about 1.1 elec-
trons. This is due to a large increase in the number of $3d$
electrons. This is compensated by a reduction in the
number of electrons on the nearest Te (4) sites and empty
(4) sites, and the net charge in the perturbed region con-
sidered here is very close to zero. An overscreening by
the Mn $3d$ electrons is not surprising, since we expect
$U_c > U$. If the core hole were screened by exactly one $3d$
electron, the effective $3d$ level would be lowered by
$U_c - U$. Considering the weak hybridization it is not
surprising that this relatively large lowering of the $3d$ lev-
el is not consistent with an increase of the $3d$ occupancy
by only one electron. A similar situation is found for Ce
(Refs. 2–4) and covalent Ni compounds.[8] For Ce com-
pounds, e.g., the lowest state in the presence of a core
hole has of the order two $4f$ electrons or more, while the
ground state without a core hole may have less than one
$4f$ electron. We find that the introduction of a core hole
reduces $\tilde{\Delta}_{3d}$ by about 17% in this calculation, including
hybridization. This is slightly less than the 22% found
by comparing the configurations $1s^1 3d^5$ with $1s^2 3d^4$ or
$1s^1 3d^6$ with $1s^2 3d^5$ in Table II, as one would expect from
the slight overscreening of the core hole in the hybridized
calculation.

## IV. CALCULATION OF THE COULOMB INTERACTION $U$

To calculate the Coulomb interaction $U$, we first set
the hopping integrals to the $3d$ orbital to zero. The
total energy $E(n_{3d\uparrow}, n_{3d\downarrow})$ and the $3d$ eigenvalue
$\varepsilon^{LD}_{3d\sigma}(n_{3d\uparrow}, n_{3d\downarrow})$ for spin $\sigma$ are then calculated as func-
tions of the occupations, $n_{3d\uparrow}$ and $n_{3d\downarrow}$, of the Mn spin-
up and spin-down orbitals, respectively. Below, we show
that $U$ can be related to the second derivative of $E$ with
respect to the $3d$ occupancy. Such a calculation of $U$ in-
cludes all the electrostatic and exchange-correlation in-
teractions of the $3d$ electrons with the valence electrons.
The system can therefore readjust the valence charge on
both the Mn and the neighboring atoms due to the
changes in the $3d$ charge. The value of $U$ is consequently
renormalized by Coulomb interactions and screening
effects not included explicitly in (1). Since the $3d$ hybridi-
zation with the valence electrons has been set to zero, $U$

is *not* renormalized by the $3d$ hopping, which is included *explicitly* in the Hamiltonian (1).

Before we deduce parameters from LSD calculations, we refer to the experience of the LSD approximation for multiplet calculations. It has been found that the LSD approximation, without any modifications, usually gives a good description of the energy of the multiplets, which can be represented as single determinants.[33] Based on this observation, a modification of the LSD approximation has been proposed which can also treat other multiplets.[33] Here we are interested in the $3d^4$, $3d^5$, and $3d^6$ configurations. For these configurations the multiplets $^5D$ ($d^4$), $^6S$ ($d^5$), and $^5D$ ($d^6$) can be represented as single determinants. From the energies of these multiplets, we obtain the energy expression

$$E(n_{3d\uparrow}, n_{3d\downarrow}) = \varepsilon_{3d} n_{3d} + \tfrac{1}{2} U n_{3d}(n_{3d} - 1)$$
$$- 0.7143(0.4 n_{3d\uparrow} - 1)$$
$$\times [F^2(3d, 3d) + F^4(3d, 3d)] \quad (41)$$

for the energy of the $3d$ electron system ($4 \leq n_{3d\uparrow} \leq 5$ and $0 \leq n_{3d\downarrow} \leq 1$), where $n_{3d} = n_{3d\uparrow} + n_{3d\downarrow}$. We have introduced the Slater integrals[34]

$$F^k(i,j) = e^2 \int_0^\infty r^2 dr [\phi_i(r)]^2$$
$$\times \int_0^\infty (r')^2 dr' [\phi_j(r')]^2 \frac{r_<^k}{r_>^{k+1}}, \quad (42)$$

where $\phi_i(r)$ is a wave function and $r_<$ ($r_>$) is the smaller (larger) of $r$ and $r'$. We now calculate the energy $E(n_{3d\uparrow}, n_{3d\downarrow})$ of the system in the LSD approximation and identify it with the expression (41). It then follows that

$$U = \frac{\partial^2 E}{\partial n_{3d}^2}. \quad (43)$$

In practice we find that slightly different results for $U$ are obtained, depending on whether the derivative in (43) is taken with respect to $n_{3d\uparrow}$ or $n_{3d\downarrow}$. We therefore use the average of these two results. From (41) we further obtain

$$\frac{\partial E(n_{3d\uparrow}, n_{3d\downarrow})}{\partial n_{3d\uparrow}} - \frac{\partial E(n_{3d\uparrow}, n_{3d\downarrow})}{\partial n_{3d\downarrow}}$$
$$= -0.2857[F^2(3d, 3d) + F^4(3d, 3d)]. \quad (44)$$

From the calculations for Mn in CdTe we deduce the value $F^2(3d, 3d) + F^4(3d, 3d) = 1.04$ Ry, which is close to the value 1.06 Ry deduced from atomic spectra.

To be able to analyze the screening of $U$ in more detail, we have also studied the effect of constraining the charge variation of the valence electrons. For instance, we have required that the number of $4s$- and $4p$-like electrons in the Mn Wigner-Seitz sphere is constant. This leads to the minimization of

$$E[n] - \lambda \int_{WS} n_{sp}(\mathbf{r}) d\mathbf{r}, \quad (45)$$

where the integral involves the integration of the charge density of $sp$ character over the Mn Wigner-Seitz sphere. The Lagrange parameter $\lambda$ is adjusted so that the desired

number of $sp$ electrons is obtained.

The numerical calculations and the analysis are simplified by using the result[35]

$$\frac{\partial E}{\partial n_i} = \varepsilon_i^{LD}, \quad (46)$$

where $n_i$ is the occupation number of a solution of the Kohn-Sham equation and $\varepsilon_i^{LD}$ is the corresponding eigenvalue. One can show that this relation is true even when a constraint of the type discussed above is introduced. Since we are using a normalized $3d$ orbital, the derivative in (46) is simply the derivative with respect to the number of $3d$ electrons. We then obtain

$$U = \frac{\partial \varepsilon_{3d\sigma}^{LD}}{\partial n_{3d\sigma}}. \quad (47)$$

It is therefore sufficient to calculate how $\varepsilon_{3d\sigma}^{LD}$ changes when the number of $3d\sigma$ electrons is varied. When the number of $3d$ electrons is increased, the eigenvalue is shifted upwards by the electrostatic potential from the added $3d$ electrons. This shift is, however, partially compensated for by a reduction in the electrostatic potential from the other electrons, which tend to move away from (screen) the Mn sphere when the $3d$ charge is increased. This reduces the value of the renormalized $U$. The calculations including the hybridization showed that the configuration with 4.9 spin-up and 0.5 spin-down $3d$ electrons gives the lowest total energy. In the absence of hybridization it is not energetically favorable to introduce holes in the $3d$ spin-up shell, which now has its full occupancy 5. For the same reason the number of spin-down $3d$ electrons is reduced from about 0.5 to 0.1. In Fig. 2 we show the change $\Delta \varepsilon_{3d}^{LD}$ of the $3d$ eigenvalue when the number of $3d$ electrons is changed. A negative change



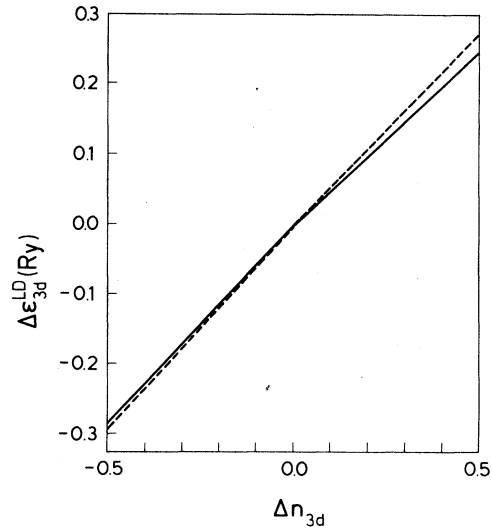FIG. 2. The change $\Delta \varepsilon_{3d}^{LD}$ of the $3d$ eigenvalue, as a function of the change $\Delta n_{3d}$ in the number of $3d$ electrons. The perturbed region included the Mn atom (dashed curve) and the Mn atom as well as the nearest-neighbor Te and empty spheres (solid curve).

means a reduction in the number of spin-up electrons and a positive change means an increase in the number of spin-down electrons relative to the configuration $3d_{\uparrow}^{5}3d_{\downarrow}^{0.1}$. The solid line shows the result when the perturbed region contains the Mn atom and the nearest-neighbor atoms and the dashed line is the result when only the Mn atom is included. The slope of the curves gives the value of $U$. The slope is slightly larger for a negative $\Delta n_{3d}$, which corresponds to a slightly larger value of $U$ for the spin-up wave function. The value of $U$ also depends weakly on the assumed size of the perturbed region. From the curves we deduce that the average value of the spin-up and spin-down $U$ is 0.57 and 0.54 Ry for the calculations with the smaller and larger perturbed regions, respectively. It is also interesting to study how the change in the number of $3d$ electrons is screened by the system. In Table IV we show the change of the charge divided by the change in the number of $3d$ electrons. About half of the $3d$ charge is screened within the Mn Wigner-Seitz sphere and more than 90% is screened within the Mn and eight nearest-neighbor spheres, and about $\frac{2}{3}$ of the charge is screened inside the Mn sphere if only the Mn sphere is assumed to be perturbed.

We now analyze the different screening mechanisms which contribute to the renormalization of the Coulomb interaction $U$. We have first performed an *atomic* calculation for the configuration $3d^{5.1}4s^{0.64}4p^{0.70}$, which is appropriate for Mn in CdTe in the absence of $3d$ hybridization. Since the curve in Fig. 2 is almost a straight line, the choice of the Mn configuration is not crucial. The results are shown in Table V. Using the atomic wave functions corresponding to the above-mentioned configuration, we obtain the electrostatic integral $F^{0}(3d,3d)\approx1.57$ Ry. This is the unrenormalized value of $U$. The $3d$ occupancy was then changed slightly and the corresponding change in the $3d$ eigenvalue was calculated self-consistently. This gives the value $U_{\text{at}}^{\text{rel}}=0.94$ Ry. The reduction of $U$ is due to the relaxation of, in particular, the $3d$, $4s$, and $4p$ orbitals, and to exchange-correlation effects. The increase of the $3d$ occupation leads to an expansion of the $3d$, $4s$, and $4p$ orbitals, and the increase in the electrostatic potential is smaller than one would deduce from the value of $F^{0}(3d,3d)$. Thus the increase in the $3d$ eigenvalue is also smaller, resulting in a reduced $U$. To quantify these arguments we proceed as follows. Let $V(\mathbf{r},n_{3d})$ be the total potential for the $3d$ occupation number $n_{3d}$. From perturbation theory it follows that

TABLE IV. The change in the charge on the central Mn site, partitioned in $l$ components, and on the neighboring four Te and four empty sites, per unit change of the number of Mn $3d$ spin-down electrons. The upper row shows a calculation when the change on the neighboring atoms was assumed to be zero.

| Mn 4s | Mn 4p | Mn 3d | Te | Empty |
|---|---|---|---|---|
| −0.33 | −0.34 | 1.00 | 0 | 0 |
| −0.24 | −0.25 | 1.00 | −0.25 | −0.19 |

$$\varepsilon_{3d}^{\text{LD}}(n_{3d}+\Delta n_{3d})-\varepsilon_{3d}^{\text{LD}}(n_{3d})$$

$$\approx\int d\mathbf{r}[\phi_{3d}(\mathbf{r})]^{2}[V(\mathbf{r},n_{3d}+\Delta n_{3d})-V(\mathbf{r},n_{3d})]\,,$$

$$(48)$$

where $\phi_{3d}$ is the $3d$ wave function calculated for the $3d$ occupation $n_{3d}$. By analyzing two self-consistent calculations, we can ascribe the difference between the two $V$'s in (48) to the change in $3d$ occupancy and to the related relaxation of the different orbitals as follows:

$$\varepsilon_{3d}^{\text{LD}}(n_{3d}+\Delta n_{3d})-\varepsilon_{3d}^{\text{LD}}(n_{3d})$$

$$=\Delta n_{3d}F^{0}(3d,3d)+\sum_{i}n_{i}[F^{0}(3d,\tilde{i})-F^{0}(3d,i)]\,,$$

$$(49)$$

where nonspherical and exchange-correlation components of the potential have been neglected. Here $i$ and $\tilde{i}$ refer to the orbitals of the atom calculated for the occupation numbers $n_{3d}$ and $n_{3d}+\Delta n_{3d}$, respectively. Combining this analysis with the definition of $U$ [Eq. (47)] we can determine how much each orbital contributes to the screening of $U$. The results are shown in Table VI. We find that the relaxation of the $3d$ orbitals themselves reduces $U$ by about 0.38 Ry and that the relaxation of the $4s$ and $4p$ orbitals gives a further reduction of about 0.16 Ry. The remaining 0.09 Ry is due to exchange-correlation effects and to the relaxation of the core orbitals. Next, we use the local neutrality assumption, in the spirit of Herring[12] and Herbst et al.[11] Thus we considered the configuration $3d^{5.1+x}4s^{0.64-x}4p^{0.70}$ and calculated $U_{\text{at}}^{\text{scr}}=\partial\varepsilon_{3d}/\partial x$. This gives $U_{\text{ac}}^{\text{scr}}=0.3$ Ry. This small value of $U$ would probably be further reduced if the atomic calculation had been replaced by a so-called re-

TABLE V. Atomic- and solid-state calculations of the $3d$ Coulomb integral $U$. The second and third rows indicate the relaxation mechanism (orbital $\phi$, or charge transfer $\rho$) taken into account. All energies are in Ry.

| Mn atom | | | Mn in CdTe | | |
|---|---|---|---|---|---|
| No relaxation | Mn | Mn | +Mn | +Te,Em | Mn,Te,Em |
| $(F^{0})$ | $\phi$ | $\phi$ | $+\rho$ | $+\rho,\rho$ | $\phi,\rho,\rho$ |
| 1.57 | 0.94 | 1.13 | 0.57 | 0.54 | 0.78 |

TABLE VI. The contributions to the atomic-orbital relaxation [Eq. (49)] of $U$ in Ry.

| No relaxation ($F^0$) | 3d | 4s,4p | Core and XC | Sum |
|---|---|---|---|---|
| 1.57 | $-0.38$ | $-0.16$ | $-0.09$ | 0.94 |

normalized atom in which the orbitals are renormalized to the Wigner-Seitz sphere, since the diffuse atomic $4s$ and $4p$ orbitals would then become more compact and the screening more efficient. Such a $U$, however, is expected to be appropriate for a metallic system but not for a semiconductor or an insulator.

The calculation described above for Mn in CdTe, yielding $U=0.54$ Ry, was analyzed as follows. First, the perturbation was assumed to be limited to the Mn sphere and we imposed the subsidiary condition that the number of $4s$ and $4p$ electrons is not changed when the number of $3d$ electrons is varied. From this calculation we deduce $U_{\text{solid}}^{\text{rel}}=1.13$ Ry (see Table V). This calculation corresponds closely to the calculation of $U_{\text{at}}^{\text{rel}}$, and the numerical value is also rather similar. We can now relax the constraint that the number of $4s$ and $4p$ electrons is fixed. This corresponds to the dashed curve in Fig. 2 and gives $U_{\text{solid}}^{\text{scr.1}}=0.57$ Ry. This number is substantially larger than $U_{\text{at}}^{\text{scr}}=0.3$ Ry, which was deduced assuming local neutrality. Actually we find that in this calculation, with only the Mn sphere perturbed, only about $\frac{2}{3}$ of the change in the $3d$ charge is screened (see Table IV). This incomplete screening is presumably a reflection of the additional energy cost in increasing the occupancy of the $4s$ and $4p$ levels caused by the presence of an energy gap, which is 1.6 eV. It would be interesting to study the screening in a system with a larger band gap or in a more ionic system, where one might expect the screening to be less efficient. Finally, we have considered the perturbed region to include also the nearest-neighbor Te and empty spheres. This corresponds to the solid curve in Fig. 2 and it gives $U_{\text{solid}}^{\text{scr.2}}=0.54$ Ry. Although the $3d$ charge is now screened to more than 90% within the perturbed region, the

reduction of $U$ compared with $U_{\text{solid}}^{\text{scr.1}}$ is marginal. The main reason is that the screening charge inside the Mn sphere is reduced from about $\frac{2}{3}$ to $\frac{1}{2}$ and that the screening on the nearest neighbors is less efficient than the screening inside the Mn sphere. To further illustrate this, we have calculated $U$ requiring that the number of $4s$ and $4p$ electrons in the Mn sphere is kept fixed but allowing the charge on the neighboring sites to adjust to the change in the number of Mn $3d$ electrons. We find that the screening charge on the neighboring atoms is much larger than in the previous calculation, where a substantial part of the screening took place in the Mn sphere. Actually, the $3d$ charge is screened to almost 90%, which is close to the number found in the calculation where the Mn $4s$ and $4p$ electrons were not constrained. The reduction of $U$ from 1.13 to 0.78 Ry is, however, substantially smaller. To understand this number we note that the distance between the Mn atom and its nearest neighbors is $d=5.3$ a.u. We then assume that the Coulomb integrals between the Mn $3d$ orbital and the nearest-neighbor orbitals are about $2/d$ Ry$\approx 0.38$ Ry. Since the screening charge is about 0.9, we expect the reduction of $U$ to be about 0.34 Ry, in close agreement with the calculations.

## V. CALCULATION OF THE CORE-$3d$ COULOMB INTERACTION $U_c$

Below we calculate the Coulomb interaction $U_c$ between a core electron and a $3d$ electron. The $1s$, $2s$, and $3s$ core electrons will be treated. As in the calculation of the Coulomb interaction $U$, we suppress the $3d$ hopping by setting the width $\tilde{\Delta}_\nu$ of the $3d$ resonance to zero. The calculations are mapped onto the energy expression

$$E(n_{c\uparrow},n_{c\downarrow},n_{3d\uparrow},n_{3d\downarrow})=\varepsilon_{3d}n_{3d}+\tfrac{1}{2}Un_{3d}(n_{3d}-1)-0.7143(0.4n_{3d\uparrow}-1)[F^2(3d,3d)+F^4(3d,3d)]$$

$$+\varepsilon_c n_c+U_c n_c n_{3d}-\tfrac{1}{5}G^2(c,3d)\sum_\sigma n_{c\sigma}n_{3d\sigma} \ . \tag{50}$$

Here $n_{c\sigma}$ and $n_{3d\sigma}$ are the occupation numbers for spin $\sigma$ of the core level and the $3d$ level, respectively, and $n_c$ and $n_{3d}$ are the corresponding total occupation numbers. The first four terms give the energy of the $3d$ electron system, as defined in (41), the fifth term describes the core-level energy, and the last two terms the interaction between the core electrons and the $3d$ electrons. $U_c$ describes the direct Coulomb interaction, and the Slater exchange integral

$$G^k(i,j)=e^2\int_0^\infty r^2 dr \int_0^\infty (r')^2 dr'\, \phi_i^*(r)\phi_j^*(r')$$

$$\times \phi_j(r)\phi_i(r')\frac{r_<^k}{r_>^{k+1}} \tag{51}$$

describes the exchange interaction.

We now consider the energy difference

$$\Delta E_\uparrow = E(c_\uparrow^1 c_\downarrow^1 3d_\uparrow^5 3d_\downarrow^1)-E(c_\uparrow^1 c_\downarrow^1 3d_\uparrow^5 3d_\downarrow^0)$$

$$-E(c_\uparrow^0 c_\downarrow^1 3d_\uparrow^5 3d_\downarrow^1)+E(c_\uparrow^0 c_\downarrow^1 3d_\uparrow^5 3d_\downarrow^0) \ . \tag{52}$$

Comparison with the energy expression (50) shows that this energy difference equals $U_c$. Using (46), we can approximate the energy difference in (52) as

$$\Delta E_\uparrow \approx \varepsilon_{3d\downarrow}^{\text{LD}}(c_\uparrow^1 c_\downarrow^1 3d_\uparrow^5 3d_\downarrow^{0.5})-\varepsilon_{3d\downarrow}^{\text{LD}}(c_\uparrow^0 c_\downarrow^1 3d_\uparrow^5 3d_\downarrow^{0.5})$$

$$\approx \frac{\partial}{\partial n_{c\uparrow}}\varepsilon_{3d\downarrow}^{\text{LD}}(c_\uparrow^{0.5} c_\downarrow^1 3d_\uparrow^5 3d_\downarrow^{0.5}) \ . \tag{53}$$

Thus we obtain

$$U_c \approx \frac{\partial}{\partial n_{c\uparrow}} \varepsilon_{3d\downarrow}^{LD}(c_\uparrow^{0.5} c_\downarrow^1 \, 3d_\uparrow^5 \, 3d_\downarrow^{0.5}) \ . \qquad (54)$$

Instead of removing a spin-up core electron as above, we can remove a spin-down core electron. This leads to the result

$$U_c - \tfrac{1}{5} G^{(2)}(c,3d) \approx \frac{\partial}{\partial n_{c\downarrow}} \varepsilon_{3d\downarrow}^{LD}(c_\uparrow^1 c_\downarrow^1 \, 3d_\uparrow^5 \, 3d_\downarrow^{0.5}) \ . \qquad (55)$$

From (54) and (55) we can deduce values for both $U_c$ and $G^{(2)}(c,d)$.

In Table VII we show results for $U_c$. The derivative in (54) was taken by making a small change in the core-level occupation number ($0.45 \to 0.55$). The column "1 shell constr." shows results of a calculation where the shapes of the orbitals in the Mn sphere are allowed to adjust to the change in the number of core electrons but no flow of charge into the Mn sphere is allowed. This calculation corresponds relatively closely to an atomic calculation. The column "1 shell" shows results of a calculation where the number of $4s$ and $4p$ electrons in the Mn sphere are allowed to adjust. We find that the change of the core charge is screened by the $4s$ and $4p$ electrons to about 70%. Since the Coulomb interaction between these states and the $3d$ state is about 0.8 Ry, we expect this screening to reduce $U_c$ by about $0.7 \times 0.8 \approx 0.6$, which is rather close to what is found. The column "3 shells" shows results where also the nearest-neighbor Te and empty spheres are allowed to screen the change in the core charge. As in the calculation of $U$, we find that this has a small effect on $U_c$. In this calculation the change in the core charge is screened to about 60% inside the Mn sphere and to about 90% within the Mn and nearest-neighbor Te and empty spheres.

Table VII shows that $U_{2s}$ is larger than $U_{1s}$. This may seem surprising for the following reasons. The unrenormalized value of $U_c$ is given by the Slater integral $F^0(c,3d)$ defined in (42). Table VIII shows that $F^0$ is larger for the $1s$ than for the $2s$ orbital, as expected from simple electrostatics: The potential at a given radius $r$ from the core orbital increases as the orbital contracts, until the orbital is located entirely inside the radius $r$ and the potential is $2/r$. The more extended $2s$ orbital has a small fraction of its tail located outside the main part of the $3d$ orbital, while this fraction is negligible for the $1s$ orbital. The $3d$ orbital, therefore, sees a slightly stronger potential from the $1s$ orbital than from the $2s$ orbital, as reflected by the values of $F^0$ in Table VIII. To under-

TABLE VII. The Coulomb interaction $U_c$ (in Ry) between a core electron and a $3d$ electron, according to a calculation where the Mn sphere and the nearest-neighbor Te and empty sphere are allowed to adjust their charge to the perturbation ("3 shell"), where only the Mn sphere adjusts its charge ("1 shell") and where in addition the number of $4s$ and $4p$ electrons in the Mn sphere is kept constant ("1 shell constr.").

| $c$ | 3 shells | 1 shell | 1 shell constr. |
|-----|----------|---------|-----------------|
| $1s$ | 0.62 | 0.64 | 1.25 |
| $2s$ | 0.70 | 0.72 | 1.31 |
| $3s$ | 0.65 | 0.67 | 1.26 |

stand why $U_{2s}$ nevertheless is larger than $U_{1s}$, we must take the relaxation of the other core orbitals into account. We have studied this in an atomic calculation. The configuration $c^{1.5} 3d^{5.5} 4s^2$ was studied, where $c$ refers to the core orbital studied and the other (solid) core orbitals are not shown explicitly. A non-spin-polarized, non-relativistic atomic program was used. We use (49) to deduce the contribution to the screening from the different orbitals. In Table VIII we show the different contributions to the shift of $\varepsilon_{3d}$ due to the creation of a core hole. When the $1s$ core hole is created, the $3s$ and $3p$ orbitals are strongly contracted. This leads to a somewhat more repulsive potential for the $3d$ level. When a $2s$ hole is created, the contraction of the $3s$ and $3p$ orbitals is smaller and the effect on the $3d$ orbital correspondingly weaker. This weaker relaxation of the $3s$ and $3p$ orbitals overcompensates for the weaker attraction of the $2s$ hole via the $F^0$ integral. This analysis neglects effects of exchange and correlation, which are, however, included in the full calculation ("Calc"). These effects are more important for the $3s$ hole, which has a larger overlap with the $3d$ state, and there is therefore a larger deviation between $\sum$ and "Calc" for the $3s$ hole than the $2s$ and $1s$ holes. Table IX shows results for the exchange integral $G^2(c,3d)$ determined from (54), and (55) and the LSD approximation. These results are compared with a direct calculation of $G^2$ from (51) using the LSD wave functions calculated for the configuration $c^{1.5} 3d^{5.5}$. The constrained one-shell calculation, where the number of $4s$ and $4p$ electrons is not allowed to vary, leads to values for $G^{(2)}(2s,3d)$ and $G^{(2)}(3s,3d)$ which are about $0.75-0.85$ of the values obtained from the direct evaluation of the Slater integral. The values of $G^{(2)}(1s,3d)$ are very small according to both methods. In contrast to the Coulomb integral $U_{cd}$, the exchange integral is screened only weakly when the number of $4s$ and $4p$ electrons is allowed to

TABLE VIII. The Slater integrals $F^0(c,3d)$ and the screening contributions from different orbitals. $\sum$ gives the net result of this analysis and "Calc" the calculated result, which includes exchange-correlation effects. All energies are in Ry and the calculations were performed for an atom with the configuration $3d^{5.5} 4s^2$.

| $c$ | $F^0(c,3d)$ | $1s + 2sp$ | $3sp$ | $3d$ | $4s$ | $\sum$ | Calc |
|-----|-------------|------------|-------|------|------|--------|------|
| $1s$ | 2.39 | $-0.04$ | $-0.36$ | $-0.80$ | $-0.25$ | 0.95 | 0.96 |
| $2s$ | 2.36 | $-0.02$ | $-0.24$ | $-0.85$ | $-0.24$ | 1.02 | 1.02 |
| $3s$ | 1.81 | $-0.00$ | $-0.08$ | $-0.54$ | $-0.23$ | 0.96 | 0.93 |

TABLE IX. The exchange integral $G^{(2)}(c,d)$ between a core electron and a $3d$ electron. The notations are the same as in Table VII. The column labeled HF (Hartree-Fock) gives the exchange integral calculated from the LSD wave functions.

| $c$ | 3 shells | 1 shell | 1 shell constr. | HF |
|-----|----------|---------|-----------------|------|
| $1s$ | 0.01 | 0.01 | 0.01 | 0.004 |
| $2s$ | 0.23 | 0.23 | 0.26 | 0.30 |
| $3s$ | 0.53 | 0.53 | 0.57 | 0.76 |

change or when the nearest-neighbor atoms can relax. The reason is that $U_{cd}$ couples to the screening charge via direct Coulomb integrals, while $G^{(2)}$ couples to the change in the spin polarization of the screening charge due to a reversal of the spin of the core hole [see (54) and (55)]. For the $3s$ core level, the predicted splitting $\frac{6}{5}G^2(3s,3d)$ (8.7 eV) between the $^7S$ and $^5S$ states is larger than the experimental value for $MnF_2$ and $MnO$ ($\sim 6$ eV).[36] The reason is a very strong interaction with an almost degenerate configuration, which leads to an anomalously large correlation effect and a reduced splitting.[37] Such an effect is clearly outside the LSD approximation. For the $2s$ level our calculated value of $G^2$, using (54) and (55) leads to an estimate (3.8 eV) of the splitting, which is smaller than the experimental splitting (5.9 eV) for $MnF_2$.[36]

## VI. PHOTOEMISSION SPECTRUM

We have performed preliminary calculations for the $3d$ photoemission spectrum, to illustrate the size of the many-body effects and to compare with experiment. The photoemission spectrum has earlier been studied theoretically by Ley et al.,[38] who used a cluster model where the $3d$ orbitals of Mn and the $5p$ orbitals of the nearest-neighbor Te atoms are included, but the other orbitals were neglected.

The calculational method for solving the Anderson model is a generalization of our earlier work[2,3] to include multiplet effects.[9,8] A many-electron basis set is constructed. For the ground-state calculation this includes a state with the Mn configuration $3d^5$ and states with six $3d$ electrons and a hole in the valence band ($3d^6v^{-1}$). For the photoemission calculation we use states with four, five, and six $3d$ electrons ($3d^4$, $3d^5v^{-1}$, and $3d^6v^{-2}$). These states are classified according to their symmetry. The multiplets of the $3d^6$ configuration can be coupled with the multiplets of the $v^{-2}$ configuration to form $3d^6v^{-2}$ states of a given symmetry in many different ways ($\sim 10^2$). We have therefore developed a computer routine for handling the symmetrization. In this calculation the coupling to the conduction band has been neglected. In view of the fairly large coupling we have found for Mn in CdTe (see Fig. 1), the effects of this approximation should be studied further.

We have used the value of $U=0.54$ Ry calculated above. For $\Delta_v(\varepsilon)$ we used the results in Fig. 1, calculated for the ground-state occupancy (5.4) of the Mn $3d$ state. In the present calculations the hopping matrix elements from a $d^n$ to a $d^{n+1}$ configuration, with $n=4,5$, are the important ones. In a future publication[39] we show that the hopping matrix elements between configurations $d^n$

and $d^{n+1}$ should be calculated for the configuration $d^{n+1}$. The configuration used here ($d^{5.4}$) is therefore not very far from the two appropriate ones. To describe the multiplet effects we also need the Slater integrals $F^2$ and $F^4$. These were estimated by fitting atomic data, since the screening effects are expected to be small for these quantities. We used the values $F^2=0.60$ Ry and $F^4=0.46$ Ry.

To determine the $3d$ level position $\varepsilon_d$, we calculate the energy cost for going from a $d^4$ to a $d^5$ configuration in the absence of hybridization. We can then determine $\varepsilon_{3d}$ from (41). From (46) it follows that the energy difference between the $d^5$ and $d^4$ configurations is approximately given by $\varepsilon_{3d}^{LD}(n_{3d}=4.5)$, where we have used the so-called transition state idea [see (46)].[35] In this way we can determine the position of the $3d$ level relative to, e.g., the top of the valence band. Since the "extended states", $\varepsilon_k$ in (1), are treated as noninteracting in the Anderson Hamiltonian, there is a need to correct their energies for the fact that the energy cost for removing one of these electrons is not equal to the energy eigenvalue in the LSD approximation. For simplicity we have, in the spirit of the transition-state concept, studied how much the Te $5p$ eigenvalue is shifted when 0.5 Te $5p$ electrons are removed, and corrected the position of $\varepsilon_d$ relative to the top of the valence band, with a large Te $5p$ character, correspondingly. The basis for this method should be further studied. In this approach we find that there is an energy gain of 0.36 Ry in going from a $d^4(^5E)$ to a $d^5(^6S)$ configuration if the extra electron is taken from the top of the valence band. This energy difference is relevant for the photoemission calculation. We further find that the "crystal-field" splitting $d^4(^5T_2)-d^4(^5E)=0.04$ Ry.

The results are compared with the experimental results of Ley et al.[38] in Fig. 3, who have subtracted off the non-$3d$ part of the spectrum. The calculated peak at about $-3$ eV is somewhat too narrow and has somewhat too much weight, but there is otherwise a rather good agreement with experiment. In particular, the combination of many-body and multiplet effects leads to the large
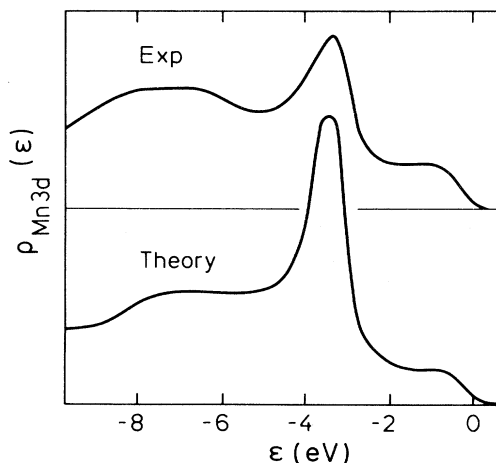


FIG. 3. The Mn $3d$ photoemission spectrum of Mn in CdTe according to experiment [Ley et al. (Ref. 38)] and theory.

observed spread of the spectrum. This is in contrast to the narrow $3d$ spectrum one would predict from a band-structure calculation. By analyzing the calculation we can deduce the character of the different parts of the spectrum. We find that the leading edge of the spectrum corresponds to states $[d^5(^6S)v^{-1}]$ with five $3d$ electrons in a $^6S$ state and a hole in the valence band. These states are similar to the ground state, except for the valence-band hole. Such a state is sometimes referred to as a delocalized hole, and it is similar to the peak at the Fermi energy in the intermetallic Ce compounds.[2,3] It corresponds to the process when a $3d$ electron is removed in the photoemission process and the $3d$ hole is filled by a valence electron close to the top of the valence band. The spectrum in the range $-3$ to $-8$ eV is a complicated mixture of final states with primarily $3d^4(^5E)$, $3d^4(^5T_2)$, $3d^5(^4T_1)v^{-1}$, and $3d^5(^4T_2)v^{-1}$ characters.

## VII. CONCLUDING REMARKS

We have presented a simple method for calculating the quantity $\Delta_v(\varepsilon)$ [see (4)], which contains all the information about the hopping integrals needed in the Anderson impurity model. The method essentially relates $\Delta_v(\varepsilon)$ to the density of states of the host and to one potential parameter ($\tilde{\Delta}_v$) for the impurity. In this approach it is not necessary to make a tight-binding fit to the band structure. Neither is it necessary to perform a tedious sum over hopping integrals to obtain the matrix element $V_{km}$, nor to perform the $k$ sum in (4). The technique does *not* rely on perturbation theory in the strength of the hopping matrix elements and it can be applied to both metals and insulators.

For Mn in CdTe we find an appreciable coupling to the conduction band, although the Te nearest neighbor have most of their weight in the valence band. The coupling in the $T_2$ symmetry is about a factor 3 larger than in the $E$ symmetry. The value of $\Delta_v(\varepsilon)$ has a strong dependence on the Mn configuration, and in particular, on the net charge. Increasing the number of $3d$ electrons by unity,

for instance, increases $\Delta_v(\varepsilon)$ by 50–60 %, and the creation of a $1s$ core hole reduces $\Delta_v(\varepsilon)$ by a factor of 2 if the number of $3d$ electrons is kept fixed. On the other hand, the creation of a core hole only reduces $\Delta_v(\varepsilon)$ by about 20% if the $3d$ electrons are allowed to screen the core hole. In a future publication[39] we show what configuration to use in the calculation of a particular matrix element.

We have also studied the screening of a localized perturbation. If all the electrons are allowed to participate in the screening, we find that for the neutral system a core hole is slightly overscreened, in spite of the semiconducting nature of the system. This is due to the efficient screening by the Mn $3d$ electrons. A change in the number of Mn $3d$ electrons is found to be screened to about 50% by the Mn $4s$ and $4p$ electrons, which screen less efficiently than the $3d$ electrons. Although this screening is less complete than what is expected for metals, it nevertheless reduces the Coulomb interaction $U$ by a factor of 2 for Mn in CdTe. It is therefore important to include this screening mechanism in the calculation of $U$. The additional inclusion of the nearest-neighbor screening has a rather small effect on $U$. The core $3d$ Coulomb integral $U_c$ is also strongly reduced by screening effects due to a charge transfer to the Mn sphere. In addition we find that the relaxation of the other core orbitals can lead to a substantial reduction of $U_c$. In particular, $U_{1s}$ is slightly smaller than $U_{2s}$ for this reason. Finally, we have found that the screening effects on the exchange integrals are small, as expected. A preliminary calculation of the photoemission spectrum using the derived parameters is in rather good agreement with experiment.

## ACKNOWLEDGMENTS

[1]P. W. Anderson, Phys. Rev. **124**, 41 (1961).

[2]O. Gunnarsson and K. Schönhammer, Phys. Rev. Lett. **50**, 604 (1983); Phys. Rev. B **28**, 4315 (1983).

[3]O. Gunnarsson and K. Schönhammer, in *Handbook on the Physics and Chemistry of Rare Earths*, edited by K. Gschneider, L. Eyring, and S. Hüfner (North-Holland, Amsterdam, 1987), Vol. 10, p. 103.

[4]J. W. Allen, S.-J. Oh, O. Gunnarsson, K. Schönhammer, M. B. Maple, M. S. Torikachvili, and I. Lindau, Adv. Phys. **35**, 275 (1987).

[5]R. Monnier, L. Degiorgi, and D. D. Koelling, Phys. Rev. Lett. **86**, 2744 (1986); L. Degiorgi, T. Greber, F. Hullinger, R. Monnier, L. Schlapbach, and B. T. Thole, Europhys. Lett. **4**, 755 (1987).

[6]O. Gunnarsson, D. D. Sarma, F. U. Hillebrecht, and K. Schönhammer, J. Appl. Phys. **63**, 3676 (1988).

[7]A. Kotani and Y. Toyozawa, J. Phys. Soc. Jpn. **35**, 1073 (1973); **37**, 912 (1974); **46**, 488 (1979).

[8]J. Zaanen, C. Westra, and G. A. Sawatzky, Phys. Rev. B **33**, 8060 (1986); G. van der Laan, J. Zaanen, G. A. Sawatzky, R. Karnatak, and J.-M. Esteva, *ibid*. **33**, 4253 (1986); G. A. Sawatzky and J. W. Allen, Phys. Rev. Lett. **55**, 418 (1985).

[9]A. Fujimori, F. Minami, and S. Sugano, Phys. Rev. B **29**, 5225 (1984).

[10]K. Schönhammer and O. Gunnarsson, Solid State Commun. **23**, 691 (1977); **26**, 399 (1978); O. Gunnarsson and K. Schönhammer, Phys. Rev. Lett. **41**, 1608 (1978).

[11]J. F. Herbst, R. E. Watson, and J. W. Wilkins, Phys. Rev. B **13**, 1439 (1976); *ibid*. **17**, 3089 (1978); J. F. Herbst and J. W. Wilkins, Phys. Rev. Lett. **43**, 1760 (1979).

[12]C. Herring, in *Magnetism*, edited by G. T. Rado and H. Suhl (Academic, New York, 1966).

[13]J. K. Lang, Y. Baer, and P. A. Cox, Phys. Rev. Lett. **42**, 74 (1979).

[14]A. Fujimori, Phys. Rev. B **28**, 2281 (1983); E. Wuilloud, B. Delly, W.-D. Schneider, and Y. Baer, Phys. Rev. Lett. **53**, 202 (1984).

[15]P. H. Dederichs, S. Blügel, R. Zeller, and H. Akai, Phys. Rev.

Lett. **53**, 2512 (1984).

[16]A. K. McMahan and R. M. Martin (unpublished).

[17]J. M. Wills and B. R. Cooper, Phys. Rev. B **36**, 3809 (1987); N. Kioussis, B. R. Cooper, and J. M. Wills, J. Appl. Phys. **63**, 3683 (1988).

[18]O. Sakai, H. Takahashi, H. Takeshige, and T. Kasuya, Solid State Commun. **52**, 997 (1984).

[19]H. Ehrenreich, Science **235**, 1029 (1987), and references therein.

[20]See, e.g., U. v. Barth and A. R. Williams, in *Theory of the Inhomogeneous Electron Gas,* edited by S. Lundqvist and N. H. March (Plenum, New York, 1983).

[21]O. K. Andersen, Phys. Rev. B **12**, 3060 (1975).

[22]O. K. Andersen and O. Jepsen, Phys. Rev. Lett. **53**, 2571 (1984); O. K. Andersen, O. Jepsen, and D. Glötzel, in *Highlights in Condensed Matter Theory,* edited by F. Bassani, F. Fumi, and M. P. Tosi (North-Holland, Amsterdam, 1985), p. 59; O. K. Andersen, Z. Pawlowska, and O. Jepsen, Phys. Rev. B **34**, 5253 (1986).

[23]A. Bringer and H. Lustfeldt, Z. Phys. B **28**, 213 (1977). A similar formula was also discussed by Wills and Cooper (Ref. 17).

[24]W. Domcke, L. S. Cederbaum, J. Schirmer, and W. von Niessen, Phys. Rev. Lett. **42**, 1237 (1979).

[25]O. Gunnarsson and K. Schönhammer, Phys. Rev. B **21**, 5863 (1980).

[26]O. Gunnarsson, O. K. Andersen, O. Jepsen, and J. Zaanen, in *Proceedings of the Tenth Taniguchi Symposium on Core-Level Spectroscopy in Condensed Systems, Kashikojima, 1987,* edited by J. Kanamori and A. Kotani (Springer, Heidelberg, 1988), p. 82.

[27]C. S. Wang, M. R. Norman, R. C. Albers, A. M. Boring, W. E. Pickett, H. Krakauer, and N. E. Christensen, Phys. Rev. B **35**, 7260 (1987).

[28]K. H. Weyrich, Phys. Rev. B **37**, 10269 (1988); H. Methfessel, *ibid.* **38**, 1537 (1988).

[29]O. Gunnarsson, O. Jepsen, and O. K. Andersen, Phys. Rev. B **27**, 7144 (1983).

[30]See, e.g., C. S. Wang and B. M. Klein, Phys. Rev. B **24**, 3393 (1981).

[31]G. Baraff and M. Schlüter, Phys. Rev. B **30**, 3460 (1984).

[32]W. Harrison, *Electronic Structure and the Properties of Solids* (Freeman, San Francisco, 1980).

[33]T. Ziegler, A. Rauk, and E. J. Baerends, Theor. Chim. Acta **43**, 261 (1977); U. von Barth, Phys. Rev. A **20**, 1963 (1979).

[34]J. C. Slater, *Quantum Theory of Atomic Structure* (McGraw-Hill, New York, 1960), Vol. 1.

[35]J. C. Slater, *Quantum Theory of Molecules and Solids* (McGraw-Hill, New York, 1974), Vol. 4; J. F. Janak, Phys. Rev. B **18**, 7165 (1978).

[36]C. S. Fadley, D. A. Shirley, A. J. Freeman, P. S. Bagus, and J. V. Mallow, Phys. Rev. Lett. **23**, 1397 (1969); C. S. Fadley and D. A. Shirley, Phys. Rev. A **2**, 1109 (1970).

[37]P. S. Bagus, A. J. Freeman, and F. Sasaki, Phys. Rev. Lett. **30**, 850 (1973).

[38]L. Ley, M. Taniguchi, J. Ghijsen, R. L. Johnson, and A. Fujimori, Phys. Rev. B **35**, 2839 (1987).

[39]O. Gunnarsson and O. Jepsen, Phys. Rev. B **38**, 3568 (1988).